CATALOGUING PERFORMANCE OF A PROPOSED EUROPEAN SPACE SITUATIONAL AWARENESS SYSTEM

Estrella Olmedo [1], Noelia Sánchez-Ortiz[2], Mercedes Ramos-Lerate[3]

[1]DEIMOS Space S.L. Ronda de Poniente 19, 2º2, Tres Cantos, Madrid, 28760 Spain, Email: estrella.olmedo@deimos-space.com

[2]DEIMOS Space S.L. Ronda de Poniente 19, 2º2, Tres Cantos, Madrid, 28760 Spain, Email: noelia.sanchez@deimos-space.com

[3]DEIMOS Space S.L. Ronda de Poniente 19, 2º2, Tres Cantos, Madrid, 28760 Spain, Email: Mercedes.ramos@deimos-space.com

ABSTRACT

In the framework of a potential European Space Situational Awareness System (ESSAS), a study of its capabilities has been done. Preliminary results for the capabilities of an ESSAS show good performances for the cataloguing operations. Performances of such system are reported in terms of observable population, timeliness of observations, system sensitivity and system redundancy.

The simulation of the features of a possible ESSAS has been done by means of the Advanced Space Surveillance System simulator (AS4) developed by DEIMOS Space, under several ESA contracts.

1. INTRODUCTION

This work is intended to the evaluation of the performances of the survey and tracking capacity of the proposed architectures for the future European Space Surveillance System. Four different phases are planned for the ESSAS set up (see [4] for requirements and preliminary definition and Table 1 for the description of assets considered in this work):

- Phase 0: Pre-Initial Operating Capability (PRE-IOC) (uses existing European assets)
- Phase 1: Initial Operating Capability (IOC)
- Phase 2: Baseline Operating Capability (BOC)
- Phase 3: Enhanced Operating Capability (EOC).

A total of 28 architectures have been analysed: 4 architectures in PRE-IOC, 8 architectures in IOC, 8 architectures in BOC; and 8 in EOC. These architectures have been split into 22 "data sets": 6 sets for LEO objects, 12 sets for GEO objects, 2 sets for MEO objects; and 2 sets for GTO objects. For every data set, the corresponding measurements have been generated by means AS4 simulator (see [2] and [3]). After that, post-process of the measurements has provided histograms, distribution functions and statistics for every data set. In order to evaluate the complete 28 architectures, we have use Figures of Merit (FOM). FOMs combine the results from data sets and provide a single mark for every architecture. Finally, the set of architectures are evaluated and compared within simple histograms where each architecture is represented by one bar.

Table 1: ESSAS assets for each phase.

	Radar assets	GB telescopes assets	SB telescopes assets	LEO	MEO	GEO	GTO
PREIOC	GRAVES TIRA	3 locations 4 for surveying (STARBROOKS (Cyprus), ZimLAT (Bern), TAROT (Chile and France)) 3 for tracking (ESASDT (Tenerife), STARBROOK North (Cyprus) and ZimSMART (Bern))	---	YES	NO	YES	NO
IOC	Survey radar in spain (step2: 10cm@1000 km) Tracking radar in Kourou	4 locations: 2 telescopes for MEO survey (6º FOV and 0.4m aperture) 4 telescopes for GEO and MEO tracking (3º FOV and 0.5m aperture) 4 additional telescopes for GEO survey (6º FOV and 0.4m aperture)	One telescope in SSO for GEO survey (10º FOV and 0.3 aperture)	YES	YES	YES	NO
BOC	Survey radar in spain (nominal: 10cm@1500 km) Tracking radar in Kourou	Same assets as IOC	Two telescopes in SSO for GEO and GTO survey (10º FOV and 0.3 aperture)	YES	YES	YES	YES
EOC	Same assets as BOC	Same assets as BOC	Same assets as BOC with one telescope in Sub-GEO (10º FOV and 0.4m aperture)	YES	YES	YES	YES

Proc. '5th European Conference on Space Debris', Darmstadt, Germany 30 March – 2 April 2009, (ESA SP-672, July 2009)

Table 3 describes the sensors used in each of these sets of simulations as well as the observation strategies. And Table 4 describes the full set of simulated architectures with the corresponding composition in data sets.

The population that will be considered for the numerical simulations has been provided by ESA (European Space Agency). Table 2 shows the definition of each type of orbit as well as the number of objects in the population with size greater than 5 cm.

Table 2:Population characteristics for the numerical simulations

Orbit Type	CONDITION	Objects (>5 cm)
LEO	Apogee < 2000 km	21,484
MEO	1.5 < Mean Motion < 2.5 rev./day Inclination < 67°	1,392
GEO	Perigee > 34000 km Apogee < 38000 km	7,964
GTO	Perigee < 2000 km 30000 < Apogee < 45000km	218
Other	Other wise	12,779
ALL	----	43,837

The final ESSAS capabilities will depend strongly on the selected observation strategies. We have based our simulations in the following previous works: [5] for the definition of GEO survey, and GEO and MEO tracking strategies in case of GB telescopes; [6] for definition of observation strategies for space based telescopes; and [7] for GB telescopes for MEO surveying.

GEO survey strategy with Ground Based (GB) telescopes: The telescope is moving in a declination strip (of –17º, 17º) at the rate of one field each 60 seconds.

MEO survey strategy with GB telescopes: The MEO survey is performed by zero declination scan over a given longitude arc (120º). The telescope pointing is moving in the longitude arc at the rate of one field each 60 seconds.

GEO and MEO tracking with GB telescopes: When the construction of the catalogue starts from scratch new objects appear continuously during the first couple of days. After these first days, the continuous appearance of new objects stops and they only happens at exceptional instances. For this reason we have also simulated the following situation: We consider the tracking telescopes dedicated exclusively to tracking tasks the first two days of simulation. And the other days, they move as GEO survey telescopes.

Observation strategy for Space Based (SB) telescopes in Sun-Synchronous Orbit (SSO) platform: We consider one Space-Based telescope located at Dawn Dusk LEO orbit pointing at two points in GEO ring, 20º apart Sun-Earth line, avoiding Earth shadow. In BOC phase two SB telescopes located in SSO are considered. The two SSO orbits are equal but with 180 degrees of difference in the true anomaly. Two situations have been simulated: One of them is dedicated to GEO survey and the other one to GTO survey (GTO observation strategy is the same than the ones for GEO objects); Both SB telescopes observe both type of orbits: GEO and GTO. In this case, each telescope points to one of the inertial point: on of them at 20º apart Sun-Earth line and the other one at -20º (avoiding the large pointing requirements at the time of pointing change).

Observation strategy for SB telescopes in sub-GEO platform: For the SB telescope located in sub-GEO platform we have considered along-track pointing.

2. EVALUATION OF ARCHITECTURES

In order to evaluate each one of the 28 architectures, the numerical results provided by the 22 data sets have been used (see Table 5).

2.1. Comparison in terms of percentage of observed objects (FOM_A)

The observed objects are the objects that have been detected during the numerical simulation by the simulated architecture. The total number of observed objects is a good indicator of the architecture capabilities as well as the effectiveness of the observation strategies. We have evaluated the number of observed objects by means of the following Figure of Merit:

$$FOM_A = \frac{1}{4}\left(aO_{LEO} + bO_{MEO} + cO_{GEO} + dO_{GTO}\right)$$

with O_{LEO}, O_{MEO}, O_{GEO} and O_{GTO} are the percentage of observed objects with respect the total number of simulated objects for objects in LEO, MEO and GEO orbits (see Table 5 for the concrete values) and *a, b, c* and *d* are weight coefficients (in PRE-IOC phase $a=c=1$, and $b=d=0$; in IOC phase $a=b=c=1$ and $d=0$; and in BOC and EOC phases $a=b=c=d=1$). Fig. 1 the numerical results for the 28 simulated architectures. Each bar corresponds to one architecture: the first bar corresponds to ARCHI_PREIOC_1, the last bar (the 28th) corresponds to ARCHI_EOC_28.

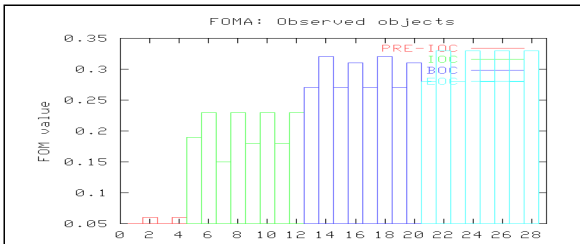

Fig. 1: Architectures performances in terms of FOM_A

In general we can observe incremental results for the incremental phases of ESSAS. Two main comments can be done. On one hand the numerical results corresponding to the architectures that use the GB tracking telescopes also for surveying in their free time (even bars) are better than the results corresponding to architecture with tracking GB telescopes dedicated only to tracking tasks (odd bars). On the other hand the numerical results, in general terms, are very poor. The maximum value of FOM_A is lower than 0,35. That is because the numerical computations have been performed with a population of 5cm. The size of this population is smaller than the required observed population (see [1]).

2.2. Comparison in terms of percentage of observable objects

The observable objects are the objects with adequate characteristics to be observed with the simulated architecture. Not all observable objects are observed. That may be due to the duration of the simulation, the particular illumination conditions, etc... The total number of observable objects is a good indicator of the architecture capabilities. We have evaluated the number of observed objects by means of the following Figure of Merit:

$$FOM_B = \frac{1}{4}\left(aB_{LEO} + bB_{MEO} + cB_{GEO} + dB_{GTO}\right)$$

with B_{LEO}, B_{MEO}, B_{GEO} and B_{GTO} are the percentage of observable objects with respect the total number of simulated objects for objects in LEO, MEO and GEO orbits (see Table 5 for the concrete values) and *a*, *b*, *c* and *d* are weight coefficients (with same values as in FOM_A).

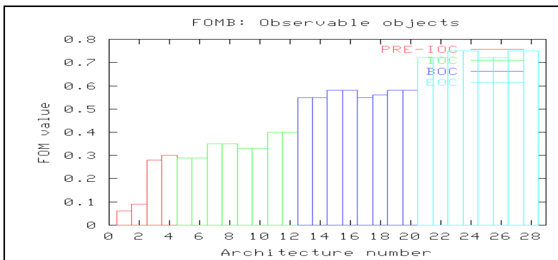

Fig. 2: Architectures performances in terms of FOM_B

Fig. 2 the numerical results. In general, we can observe incremental results for the incremental phases of ESSAS. As in case of FOM_A, FOM_B reflects also the incremental capabilities of those architectures with GB tracking telescopes used also for surveying. Main difference between FOM_A and FOM_B is that, FOM_B provides better performances. The 80% of population of 5 cm is observable with the architecture, but only the 30% of objects are really observed. Let us explain this fact. On one hand, the 80% of the population is observable when we consider a SB telescope in sub-GEO platform. The SB telescope is very close to GEO ring and therefore, it can observe very small objects. The problem with the use of that telescopes is that the sinodic period of the GB telescope in sub-GEO and an object in the GEO ring is very high. And therefore, a numerical simulation of 30 days is not significant. Longer numerical simulations must be performed for observing all the observable objects from sub-GEO platform. On the other hand the number of observable objects increase when a tracking radar is considered in the architecture (radar tracking may observe more objects than survey radar), however, the number of observed objects comes from the observations from survey radar. Tracking radar is used only (in our simulations) for tracking observed objects from survey radar. Moreover the observation strategy in case of telescopes plays also a relevant role. Good observations strategies may observe the majority of observable objects. However, when the strategy is not optimal, the number of observed objects is much lower than the number of observable objects. Most of the observation strategies are not yet defined (see [4]). A more extensive study of observation strategies is out of scope of this work

2.3. Comparison in terms of coverage of observed objects

The coverage system evaluates the maximum re-observation period of the already catalogued objects. The lower the re-observation period, better the orbital determination capabilities and therefore better conditions for maintaining a catalogue. We consider FOM_1 (already defined in [1]) in order to evaluate the coverage system:

$$FOM_1 = \frac{1}{4}\left(aP_{LEO} + bP_{MEO} + cP_{GEO} + dP_{GTO}\right)$$

with P_{LEO}, P_{MEO}, P_{GEO} and P_{GTO} are the percentage of observed objects correctly maintained in LEO, MEO, GEO and GTO orbits and and *a*, *b*, *c* and *d* are weight coefficients (with same values as in FOM_A).

Fig. 3 shows the numerical results. In general we can observe incremental result for the incremental phases of ESSAS. We want to remark that the results corresponding to EOC phase are much better than the numerical results that will be obtained in the operational case. In EOC phase has been considering one SB telescope in sub-GEO platform. This telescope allows detecting very small objects that cannot be detected from the other sensors of the architecture (the SB telescopes in SSO or/and the tracking GB telescopes). Those so small objects will be observed only from SB telescope in sub-GEO platform. But the re-observation period in this case is very high (up to two months). In our simulations this behavior is not observed because the numerical simulation has been performed during 30 days only. For this reason, for practical purposes, the better results in terms of FOM1are obtained with ARCHI_BOC_17 and ARCHI_BOC_19. These architectures correspond to considering two SB telescopes in SSO for observing GEO and GTO objects. Both architectures have the same numerical results because the difference between then is the tracking radar (ARCHI_BOC_19 contains one tracking radar and ARCHI_BOC_17 does not) that for computation of FOM1 does not affect.

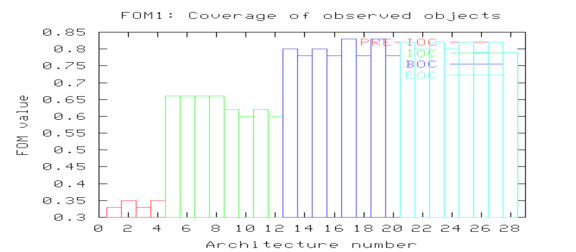

Fig. 3: Architectures performances in terms of FOM_1

2.4. Comparison in terms of coverage of simulated objects

We consider here a modification of FOM_1. The formulation of FOM_{1b} is the same as the formulation of FOM_1. The only difference is that the percentage of correctly maintained objects is not computed over the set of observed objects, but over the set of simulated objects.

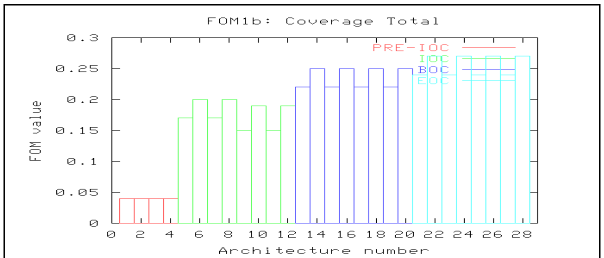

Fig. 4: Architectures performances in terms of FOM_{1b}

Fig. 4 shows the numerical results. In general we can observe incremental result for the incremental phases of ESSAS. As for FOM1, the numerical results corresponding to EOC phase will be worse than the simulated one due to the high re-observation period for SB telescopes in sub-GEO platform. We want to comment two things:

- As one could expect, the numerical results reflect better performances when GB tracking telescopes are used also for surveying (even bars in histogram of Fig. 4). This incremental behaviour is not observed in Fig. 3 because the percentage is not computed over the total set of simulated objects.
- The numerical results in IOC phase (green bars) show better performances for the architectures with GB telescopes for surveying GEO objects (bars: 5,6, 7 and 8) than for architectures with SB telescope in SSO (bars 9, 10, 11 and 12). In BOC this behaviour is not observed because radar capabilities increase and GTO objects are observed. Therefore the total computation makes FOM1b higher than for architectures with GB telescopes only. The inconvenience of having only GB telescopes is that adverse weather conditions may avoid many nights of observations.

2.5. Comparison in terms of survey timeliness

The survey timeliness is the time between a new object appearing and a survey sensor detecting it. We consider FOM_9 (already defined in [1]) in order to evaluate the survey timeliness system.

$$FOM_9 = \left(aT_{LEO} + \frac{b}{7}T_{MEO} + \frac{c}{7}T_{GEO} \right)^{-1}$$

with T_{LEO}, T_{MEO} and T_{GEO} are the mean time from new object appearing and first measurement for objects in LEO, MEO and GEO orbits and *a*, *b*, *c* and *d* are weight coefficients (in PRE-IOC phase $a=c=1$, and $b=0$; in IOC, BOC and EOC phase $a=b=c=1$. Fig. 5 shows the numerical results. Let us comment briefly the obtained results. On one hand the better results correspond to ARCHI_IOC_5 and ARCHI_IOC_7. These architectures contain GB telescopes only for surveying GEO objects. That means that the coverage obtained with four GB telescopes in the selected four sites is optimal for surveying GEO objects (in our computations has not been considered adverse weather conditions). On the other hand, the numerical results obtained for EOC phase are very poor. That is due to the SB telescope in sub-GEO platform. The objects observed only from sub-GEO platform, may be detected up to 2 months after their appearance.

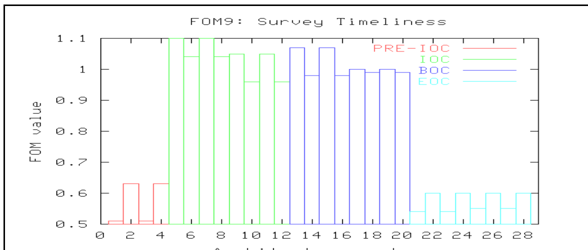

Fig. 5: Architectures performances in terms of FOM_9

2.6. Comparison in terms of tracking timeliness

The tracking timeliness is the time between an user request of observing an object and a tracking sensor availability of observing it. We consider FOM_{10} (already defined in [1]) in order to evaluate the tracking timeliness system:

$$FOM_{10} = \frac{1}{3}(a(1-T_{LEO}) + b(1-T_{MEO}/2) + c(1-T_{GEO}/4))$$

with T_{LEO}, T_{MEO} and T_{GEO} are the mean time from new object is detected by a survey sensor and a tracking sensor detects it for objects in LEO, MEO and GEO orbits and *a*, *b*, *c* and *d* are weight coefficients (with same values as in FOM_9).

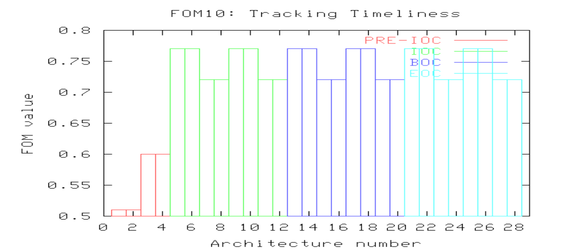

Fig. 6: Architectures performances in terms of FOM_{10}

Fig. 6 shows the numerical results. The numerical results for IOC, BOC and EOC phases are always the same because the tracking sensors are equal. We want to comment that we observe worse results for those architectures that use the new tracking radar (results corresponding to bars: 7, 8, 11, 12, 15, 16, 19, 20, 23, 24, 27 and 28). That is due to the location of the new tracking radar. The latitude of the tracking radar (Kourou) is lower than the latitude of the survey radar (Spain). The reaction time increases when the latitude of the radar decreases. Therefore the corresponding performances are worse.

2.7. Comparison in terms of sensitivity system

The sensitivity of the system consists in computing the minimum diameter detected by the sensors of the architecture. We consider FOM_6 (already defined in [1]) in order to evaluate the sensitivity system:

$$FOM_6 = \left(\frac{a}{10}D_{LEO} + \frac{b}{100}D_{MEO} + \frac{c}{100}D_{GEO}\right)^{-1}$$

with D_{LEO}, D_{MEO} and D_{GEO} are the minimum detectable size for objects in LEO, MEO and GEO orbits and *a*, *b*, *c* and *d* are weight coefficients (with same values as in FOM_9).

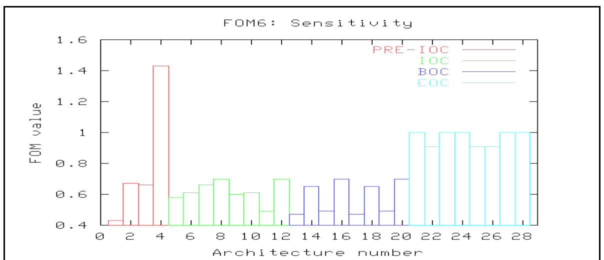

Fig. 7: Architectures performances in terms of FOM_6

Fig. 7 shows the numerical results The most spectacular result is the one obtained with ARCHI_PREIOC_4. This architecture contains TIRA radar. We want to remark that we have computed the minimum detectable size for GB and SB telescopes as the minimum detectable size observed with survey sensors. ARCHI_PREIOC_2 also contains TIRA radar and the corresponding bar is not so big as the 4th bar. That is due to the minimum GEO detectable size is 109 cm because the tracking GB telescopes are not considered in this computation. In ARCHI_PREIOC_4, since the tracking GB telescopes are also used for surveying, the minimum detectable GEO size is 49 cm. The architectures in EOC phase also provide very good results of FOM_6. In those architectures, a SB telescope in sub-GEO platform is considered. That telescope allows detecting GEO objects up to 5 cm (in our simulated population greater than 5cm).

2.8. Comparison in terms of redundancy system

The redundancy says if some fraction of each orbital region is covered by more than one sensor. We have evaluated the redundancy system by means of the following Figure of Merit:

$$FOM_C = \frac{1}{4}\left(aR_{LEO} + bR_{MEO} + cR_{GEO} + dR_{GTO}\right)$$

with R_{LEO}, R_{MEO}, R_{GEO} and R_{GTO} are the percentage of redundancy in LEO, MEO, GEO and GTO orbits and and *a*, *b*, *c* and *d* are weight coefficients (with same values as in FOM_A).Fig. 8 shows the numerical results.

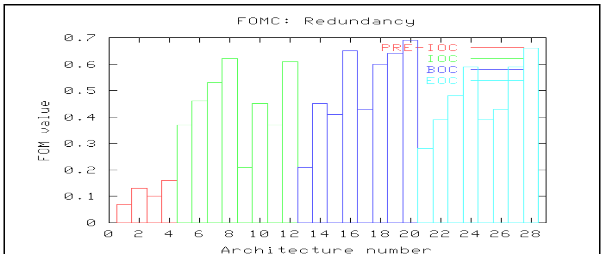

Fig. 8: Architectures performances in terms of FOM_C

3. GENERAL CONCLUSIONS

Evaluation of architecture from FOMS: We have evaluated the architectures by means of several Figures of Merit. Some of them have been previously defined in [1]. These FOMS assign to each aspect to be evaluated of architecture a mark. In such a way that the comparison between each architecture can be performance by means of histograms.

Tracking radar: The best results for the simulated tracking radars correspond to TIRA. The main inconvenience of this radar is that its availability is not yet ensured. For this reason it has been proposed constructing new tracking radar.

GB telescopes versus SB telescopes for GEO surveying: The performances of simulated GB telescopes are better than the performances of simulated SB telescopes in SSO. A good ground based system of telescopes may provide better performances than one telescope only in SSO. This result is subjected to several conditions. On one hand the GB telescopes have the inconvenience of the weather conditions. On the other hand, the simulated SB telescopes have bigger FOV but smaller aperture than the simulated GB telescopes (i.e. do not detect so smaller objects). By improving the technical characteristics of the SB telescopes the corresponding performances will improve.

SB telescope in sub-GEO platform for GEO survey: The inclusion of only one SB telescope in sub-GEO platform, dedicated to surveying the GEO ring, does not present advantages. Although smaller GEO objects may be detected, the revisit period for those objects observed only by sub-GEO platform will be very high. Therefore the orbital determination will become very poor and the correlation of them will be very complicated. The way of solving this fact is to considering a constellation of equidistant telescopes in sub-GEO platforms. Otherwise, these telescopes are not suitable at all for surveying GEO ring.

GB tracking telescopes used also for surveying in their free time: The appearance of new objects does not occur in a continuous way. In particular when the construction of the catalogue starts from scratch they appear continuously during the first couple of days (that is because; we are considering telescopes with fast CDD and big FOV, therefore, the declination strip can be covered in 12 minutes (12 field, one field each minute)). After these first days, the appearance of new objects stops and they only happens at exceptional instances. For this reason, we propose considering the tracking telescopes not exclusively for tracking tasks but also for surveying.

Observation strategies: In general, adequate observation strategies are required for obtained proper architecture capabilities. Observation strategies for MEO and GTO survey must be defined (and previously studied). Moreover the 29% of the simulated population (greater than 5cm) corresponds to Other type of orbit. This population must be also taking into account in future works.

Architectures appropriated for population with objects >10cm: In general the performances of the simulated architectures seem to be adequate for Space Debris population greater than 10cm. However, for population of objects greater than 5 cm the architecture capabilities seem to be insufficient.

AS4 simulator: The analysis performed in this work has been completely performed by means of the Advanced Space Surveillance System simulator (AS4) developed by DEIMOS Space, under several ESA contracts (see [2], [3] and [8]).

4. REFERENCES

[1] Saunders, C, Analysis of User Needs, ESA Contract 21270/07/NL/ST, QinetiQ, March 2008

[2] Tresaco, E., Sánchez-Ortiz, N., Belló, M., Martín, J.F., Marchesi, J.E., Pina, F., "*Advanced Space Surveillance System Simulator*", Final Report of ESOC Contract No. 18687/04/D/HK (SC), Deimos Space S.L., 10/03/2006

[3] Olmedo-Casal, E., Sánchez-Ortiz, N., Ramos-Lerate, M., Belló-Mora, M. "*Design & Development of Space Surveillance System Catalogue Correlation Techniques*", Final Report of ESA/ESTEC Study Contract No. 20070/06/NL/HE, 19/12/2007

[4] Saunders, C, Development and trade-off of candidate architecture concept options, ESA Contract 21270/07/NL/ST, QinetiQ, December 2008

[5] E. Olmedo, N. Sánchez-Ortiz, M. R. Belló-Mora, H. Klinkrad, F. Pina, "Initial Orbit Determination algorithms for cataloguing optical measurements of Space Debris", Monthly Notices of the Royal Astronomic Society, Vol. 391, pag 1259-1272, (2008)

[6] N. Sánchez-Ortiz, E. Olmedo, M. R-Lerate, E. M. Perez: Space Based Optical Images within a Space Surveillance System, Proceedings of the International Astronautical Congress 2008 (IAC-08-A6.5.6)

[7] T. Flohrer, T. Schildknecht, R. Musci, "*Proposed strategies for optical observations in a future European Space Surveillance Network*", presented in the 36th COSPAR Scientific Assembly (2006).

[8] E. Olmedo, N. Sánchez-Ortiz, M. R. Lerate, M. Belló-Mora, H. Klinkrad, "Design and Development of correlation techniques to maintain a Space Surveillance System Catalogue", accepted at Acta Astronautica. DOI: 10.1016/j.actaastro.2009.03.024 PII: S0094576509001817

5. ANNEX1: ADDITIONAL TABLES

Table 3: Simulation sets description

Simulation Sets	**Type of Orbit**	[illegible]	**Considered sensors**
LEO_SET_1	L E O	7	1 radar: GRAVES
LEO_SET_2	L E O	[illegible]	2 radar: GRAVES +TIRA
LEO_SET_3	L E O	7	1 radar: survey step 2
LEO_SET_4	L E O	[illegible]	2 radar: survey step 2 + tracking
LEO_SET_5	L E O	7	1 radar: survey nominal
LEO_SET_6	L E O	[illegible]	2 radar: survey nominal + tracking
GEO_SET_7	G E O	30	STARBROOK, ZimSMART and TAROT (Chile and France) for STARBROOK north, ZimLAT and ESASDT for GEO tracking
GEO_SET_8	G E O	[illegible]	STARBROOK, ZimSMART and TAROT (Chile and France) for GEO survey STARBROOK north, ZimLAT and ESASDT for GEO tracking (tracking

			telescopes make survey in free time)
GEO_SET_9	G E O	3 0	4 telescopes for GEO survey 4 telescopes for MEO and GEO tracking
GEO_SET_10	G E O	[illegible]	4 telescopes for GEO survey 4 telescopes for MEO and GEO tracking (the tracking telescopes makes also survey in free time)
GEO_SET_11	G E O	3 0	1 space based telescope in SSO platform for GEO survey 4 telescopes for MEO and GEO tracking
GEO_SET_12	G E O	[illegible]	1 space based telescope in SSO platform for GEO survey 4 telescopes for MEO and GEO tracking (the tracking telescopes makes also survey in free time)
GEO_SET_13	G E O	3 0	2 Space Based Telescope in SSO for GTO, HEO and GEO surveying 4 telescopes for MEO and GEO tracking
GEO_SET_14	G E O	[illegible]	2 Space Based Telescope in SSO for GTO, HEO and GEO surveying 4 telescopes for MEO and GEO tracking (the tracking telescopes makes also survey in free time)
GEO_SET_15	G E O	3 0	1 space based telescope in SSO platform for GEO survey 4 telescopes for MEO and GEO tracking 1 space based telescope for GEO survey in sub-GEO platform
GEO_SET_16	G E O	[illegible]	1 space based telescope in SSO platform for GEO survey 4 telescopes for MEO and GEO tracking (the tracking telescopes makes also survey in free time) 1 space based telescope for GEO survey in sub-GEO platform
GEO_SET_17	G E O	3 0	2 Space Based Telescope in SSO for GTO, HEO and GEO surveying 4 telescopes for MEO and GEO tracking 1 space based telescope for GEO survey in sub-GEO platform
GEO_SET_18	G E O	[illegible]	2 Space Based Telescope in SSO for GTO, HEO and GEO surveying 4 telescopes for MEO and GEO tracking (the tracking telescopes makes also survey in free time) 1 space based telescope for GEO survey in sub-GEO platform
MEO_SET_19	ME O	3 0	2 telescopes for MEO survey 4 telescopes for MEO and GEO tracking
MEO_SET_20	ME O	[illegible]	2 telescopes for MEO survey 4 telescopes for MEO and GEO tracking (the tracking telescopes makes also survey in free time)
GTO_SET_21	G T O	3 0	1 Space Based Telescope in SSO for GTO and HEO surveying
GTO_SET_22	G T O	[illegible]	2 Space Based Telescope in SSO for GTO, HEO and GEO

Table 4: Simulated architectures composition

Simulated architecture	Composition of simulation sets	Number of each type of sensors	
ARCHI_PREIOC_1	LEO_SET_1 + GEO_SET_7	Radars	1
		GB telescopes	7
		SB telescopes	0
ARCHI_PREIOC_2	LEO_SET_1 +	Radars	1
		GB telescopes	7
		SB telescopes	0
ARCHI_PREIOC_3	LEO_SET_2 + GEO_SET_7	Radars	2
		GB telescopes	7
		SB telescopes	0
ARCHI_PREIOC_4	LEO_SET_2 + GEO_SET_8	Radars	2
		GB telescopes	7
		SB telescopes	0
ARCHI_IOC_5	LEO_SET_3 + GEO_SET_9 + MEO_SET_19	Radars	1
		GB telescopes	10
		SB telescopes	0
ARCHI_IOC_6	LEO_SET_3 + GEO_SET_10 + MEO_SET_20	Radars	1
		GB telescopes	10
		SB telescopes	0
ARCHI_IOC_7	LEO_SET_4 + GEO_SET_9 + MEO_SET_19	Radars	2
		GB telescopes	10
		SB telescopes	0
ARCHI_IOC_8	LEO_SET_4 + GEO_SET_10 + MEO_SET_20	Radars	2
		GB telescopes	10
		SB telescopes	0
ARCHI_IOC_9	LEO_SET_3 + GEO_SET_11 + MEO_SET_19	Radars	1
		GB telescopes	6
		SB telescopes	1
ARCHI_IOC_10	LEO_SET_3 + GEO_SET_12 + MEO_SET_20	Radars	1
		GB telescopes	6
		SB telescopes	1
ARCHI_IOC_11	LEO_SET_4 + GEO_SET_11 + MEO_SET_19	Radars	2
		GB telescopes	6
		SB telescopes	1
ARCHI_IOC_12	LEO_SET_4 + GEO_SET_12 + MEO_SET_20	Radars	2
		GB telescopes	6
		SB telescopes	1
ARCHI_BOC_13	LEO_SET_5 + GEO_SET_11+ MEO_SET_19 + GTO _SET_21	Radars	1
		GB telescopes	6
		SB telescopes	2
ARCHI_BOC_14	LEO_SET_5 + GEO_SET_12 + MEO_SET_20 + GTO _SET_21	Radars	1
		GB telescopes	6
		SB telescopes	2
ARCHI_BOC_15	LEO_SET_6 + GEO_SET_11 + MEO_SET_19 + GTO _SET_21	Radars	2
		GB telescopes	6
		SB telescopes	2
ARCHI_BOC_16	LEO_SET_6 + GEO_SET_12 + MEO_SET_20 + GTO _SET_21	Radars	2
		GB telescopes	6
		SB telescopes	2
ARCHI_BOC_17	LEO_SET_5 + GEO_SET_13 + MEO_SET_19 + GTO _SET_22	Radars	1
		GB telescopes	6
		SB telescopes	2
ARCHI_BOC_18	LEO_SET_5 + GEO_SET_14 + MEO_SET_20 + GTO _SET_22	Radars	1
		GB telescopes	6
		SB telescopes	2
ARCH _BOC_19	LEO_SET_6 + GEO_SET_13 + MEO_SET_19 + GTO _SET_22	Radars	2
		GB telescopes	6
		SB telescopes	2
ARCHI_BOC_20	LEO_SET_6 + GEO_SET_14 + MEO_SET_20 + GTO_SET_22	Radars	2
		GB telescopes	6
		SB telescopes	2
ARCHI_EOC_21	LEO_SET_5 + GEO_SET_15 + MEO_SET_19 + GTO _SET_20	Radars	1
		GB telescopes	6
		SB telescopes	3
ARCHI_EOC_22	LEO_SET_5 + GEO_SET_16 +	Radars	1
		GB telescopes	6

		MEO_SET_20 + GTO _SET_21	SB telescopes	3
	ARCHI_EOC_23	LEO_SET_6 + GEO_SET_15 + MEO_SET_19 + GTO_ SET_21	Radars	2
			GB telescopes	6
			SB telescopes	3
	ARCHI_EOC_24	LEO_SET_6 + GEO_SET_16 + MEO_SET_20 + GTO_ SET_21	Radars	2
			GB telescopes	6
			SB telescopes	3
	ARCHI_EOC_25	LEO_SET_5 + GEO_SET_17 + MEO_SET_19 + GTO_ SET_22	Radars	1
			GB telescopes	6
			SB telescopes	3
	ARCHI_EOC_26	LEO_SET_5 + GEO_SET_18 + MEO_SET_20 + GTO_ SET_22	Radars	1
			GB telescopes	6
			SB telescopes	3
	ARCHI_EOC_27	LEO_SET_6 + GEO_SET_15 + MEO_SET_17 + GTO_ SET_20	Radars	2
			GB telescopes	6
			SB telescopes	3
	ARCHI_EOC_28	LEO_SET_6 + GEO_SET_16 + MEO_SET_18 + GTO_ SET_20	Radars	2
			GB telescopes	6
			SB telescopes	3

Table 5: Numerical results for data sets

DATA SET	SIMU-LATED OBJECTS	OBSER-VABLE	OBSERVED
LEO_SET_ 1	21484	2708	2701
LEO_SET_ 2	21484	21150	2701
LEO_SET_ 3	21484	9685	9333
LEO_SET_ 4	21484	15300	9333
LEO_SET_ 5	21484	12357	11949
LEO_SET_ 6	21484	15300	11949
GEO_SET_7	7964	929	615
GEO_SET_8	7964	1773	857
GEO_SET_9	7964	1033	1023
GEO_SET_10	7964	1071	1062
GEO_SET_11	7964	2376	827
GEO_SET_12	7964	2376	1062
GEO_SET_13	7964	2376	836
GEO_SET_14	7964	2376	1062
GEO_SET_15	7964	7788	1305
GEO_SET_16	7964	7788	1447
GEO_SET_17	7964	7788	1310
GEO_SET_18	7964	7788	1447
MEO_SET_19	1392	780	469
MEO_SET_20	1392	784	494
GTO_ SET_21	218	166	46
GTO_ SET_22	218	166	45
DATA SET	**Percentage of observed objects correctly maintained**	**Minimum Observed Diameter (m)**	**Percentage of simulated objects correctly maintained**
LEO_SET_ 1	87%	0.13	10.94%
LEO_SET_ 2	87%	0.05	10.94%
LEO_SET_ 3	90%	0.07	39.18%
LEO_SET_ 4	90%	0.05	39.18%
LEO_SET_ 5	91%	0.06	50.62%
LEO_SET_ 6	91%	0.05	50.62%
GEO_SET_7	46%	1.02	3.6%
GEO_SET_8	53%	0.20	5.7%
GEO_SET_9	99%	0.56	12.72%
GEO_SET_10	96%	0.49	12.80%
GEO_SET_11	83%	1.09	8.62%
GEO_SET_12	71%	0.49	9.47%
GEO_SET_13	97%	1.09	10.18%
GEO_SET_14	73%	0.49	10.18%
GEO_SET_15	89%	0.05	14.26%
GEO_SET_16	79%	0.05	14.26%
GEO_SET_17	93%	0.05	15.30%
GEO_SET_18	80%	0.05	15.30%
MEO_SET_19	73%	0.45	13.86%
MEO_SET_20	77%	0.45	25.81%
GTO_ SET_21	71%	0.14	14.95%
GTO_ SET_22	68%	0.07	14.04%
DATA SET	**System redundancy**	**Survey Timeliness (h)**	**Tracking Timeliness (h)**
LEO_SET_ 1	0%	9.262	9.262
LEO_SET_ 2	11.53%	9.262	2.491
LEO_SET_ 3	0%	7.997	7.997
LEO_SET_ 4	64.07%	7.997	11.558
LEO_SET_ 5	0%	7.349	7.349
LEO_SET_ 6	81.86%	7.349	11.558
GEO_SET_7	26.67%	262.959	8.413
GEO_SET_8	50.29%	201.924	8.413
GEO_SET_9	65%	16.534	10.367
GEO_SET_10	98.96%	18.094	10.367
GEO_SET_11	0%	23.130	10.367
GEO_SET_12	94.82%	31.878	10.367
GEO_SET_13	72.85%	21.402	10.367
GEO_SET_14	95.01%	29.505	10.367
GEO_SET_15	28.35%	178.484	10.367
GEO_SET_16	70.56%	140.913	10.367
GEO_SET_17	56.26%	173.895	10.367
GEO_SET_18	70.63%	138.757	10.367
MEO_SET_19	82.52%	81.563	12.48
MEO_SET_20	84.12%	87.318	12.48
GTO_ SET_21	0%	169.96	169.96
GTO_ SET_22	15.91%	147.463	147.463